

Observational Study

Incidental congenital coronary artery vascular fistulas in adults: Evaluation with adenosine-¹³N-ammonia PET-CT

Salah AM Said, Aly Agool, Arno HM Moons, Mounir WZ Basalus, Nils RL Wagenaar, Rogier LG Nijhuis, Jutta M Schroeder-Tanka, Riemer HJA Slart

Salah AM Said, Mounir WZ Basalus, Rogier LG Nijhuis, Department of Cardiology, Hospital Group Twente, Almelo-Hengelo 7555 DL, Overijssel, The Netherlands

Aly Agool, Nils RL Wagenaar, Department of Nuclear Medicine, Hospital Group Twente, Almelo-Hengelo 7555 DL, Overijssel, The Netherlands

Arno HM Moons, Department of Cardiology, Slotervaart Hospital, Amsterdam 1066 EC, North Holland, The Netherlands

Jutta M Schroeder-Tanka, Department of Cardiology, Hospital Onze Lieve Vrouwe Gasthuis, Location West, Amsterdam 1061 AE, North Holland, The Netherlands

Riemer HJA Slart, Medical Imaging Center, Department of Nuclear Medicine and Molecular Imaging, University Medical Center Groningen, Groningen 9713 GZ, The Netherlands

Riemer HJA Slart, Faculty of Science and Technology, Biomedical Photonic Imaging, University of Twente, Enschede 7522 NB, The Netherlands

ORCID number: Salah AM Said (0000-0003-1221-9264); Aly Agool (0000-0003-1644-3597); Arno HM Moons (0000-0003-0647-9772); Mounir WZ Basalus (0000-0002-7008-5973); Nils RL Wagenaar (0000-0003-3966-1140); Rogier LG Nijhuis (0000-0001-6975-8053); Jutta M Schroeder-Tanka (0000-0001-5962-3286); Riemer HJA Slart (0000-0002-5565-1164).

Author contributions: All authors contributed to this paper; concept and design by Said SAM and Basalus MWZ; data acquisition by Moons AHM, Schroeder-Tanka JM and Nijhuis RLG; analysis of nuclear studies Agool A, Wagenaar NRL and Slart RHJA; Slart RHJA performed critical revision of manuscript; all authors have approved the final version of the paper.

Institutional review board statement: The study was reviewed and approved by the local medical ethical committee of the Eastern region, Enschede, The Netherlands (ID METC: K18-14, METC/18082.sai).

Informed consent statement: The study was reviewed and approved by the local medical ethical committee and the requirement to obtain informed consent was waived due to the retrospective nature of the report, the Eastern region, Enschede, The Netherlands (ID METC: K18-14, METC/18082.sai).

Conflict-of-interest statement: The authors declare that they have no competing interests.

STROBE statement: The authors have read the STROBE Statement-checklist of items, and the manuscript was prepared and revised according to the STROBE Statement-checklist of items.

Open-Access: This article is an open-access article which was selected by an in-house editor and fully peer-reviewed by external reviewers. It is distributed in accordance with the Creative Commons Attribution Non Commercial (CC BY-NC 4.0) license, which permits others to distribute, remix, adapt, build upon this work non-commercially, and license their derivative works on different terms, provided the original work is properly cited and the use is non-commercial. See: <http://creativecommons.org/licenses/by-nc/4.0/>

Manuscript source: Invited manuscript

Correspondence to: Salah AM Said, MD, PhD, Doctor, Staff Physician, Cardiologist, Department of Cardiology, Hospital Group Twente, Geerdinksweg 141, Almelo-Hengelo 7555 DL, Overijssel, The Netherlands. samsaid@home.nl
Telephone: +31-88-7085286
Fax: +31-88-7085289

Received: June 27, 2018
Peer-review started: June 30, 2018
First decision: July 19, 2018
Revised: August 21, 2018
Accepted: August 30, 2018
Article in press: August 30, 2018
Published online: October 26, 2018

Abstract

AIM

To assess the functionality of congenital coronary artery fistulas (CAFs) using adenosine stress ¹³N-ammonia positron emission tomography computed tomography (PET-CT).

METHODS

Congenital CAFs were incidentally detected during coronary angiography (CAG) procedures in 11 adult patients (six males and five females) with a mean age of 64.3 years (range 41-81). Patients were collected from three institutes in the Netherlands. The characteristics of the fistulas (origin, pathway and termination), multiplicity of the origins and pathways of the fistulous vessels were assessed by CAG. Five patients underwent adenosine pharmacologic stress ¹³N-ammonia PET-CT to assess myocardial perfusion and the functional behavior of the fistula.

RESULTS

Eleven patients with 12 CAFs, 10 unilateral and one bilateral, originating from the left anterior descending coronary artery ($n = 8$), right coronary artery ($n = 2$) and circumflex ($n = 2$). All fistulas were of the vascular type, terminating into either the pulmonary artery ($n = 11$) or coronary sinus ($n = 1$). The CAG delineated the characteristics of the fistula (origin, pathway and termination). Multiplicity of the origins and pathways of the fistulous vessels were common in most fistulas (8/12, 67% and 9/12, 75%, respectively). Multiplicity was common among the different fistula components (23/36, 64%). Adenosine pharmacologic stress ¹³N-ammonia PET-CT revealed normal myocardial perfusion and ejection fraction in all but one patient, who showed a reduced ejection fraction.

CONCLUSION

PET-CT may be helpful for assessing the functional status of congenital CAFs in selected patients regarding clinical decision-making. Studies with a larger patient series are warranted.

Key words: Coronary angiography; Coronary-pulmonary artery fistulas; Adenosine ammonia positron emission tomography computed tomography; Coronary vascular fistulas; Congenital coronary artery fistulas

© **The Author(s) 2018.** Published by Baishideng Publishing Group Inc. All rights reserved.

Core tip: Congenital coronary artery fistulas are usually detected as a coincidental finding during non-invasive and invasive diagnostic modalities for the assessment of coronary artery disease. Positron emission tomography computed tomography (PET-CT) is not frequently applied for functional assessment. In the current study, five patients underwent adenosine ¹³N-ammonia PET-CT to assess myocardial perfusion and the functional behavior of the fistula. PET-CT revealed normal myocardial per-

fusion and ejection fraction in all but one patient, who showed a reduced ejection fraction. Combined with semi-quantitative results, patients with normal flow, revealed by PET-CT, could be treated medically, thereby avoiding the need for transcatheter or surgical occlusion of the fistulas.

Said SAM, Agoon A, Moons AHM, Basalus MWZ, Wagenaar NRL, Nijhuis RLG, Schroeder-Tanka JM, Slart RHJA. Incidental congenital coronary artery vascular fistulas in adults: Evaluation with adenosine-¹³N-ammonia PET-CT. *World J Cardiol* 2018; 10(10): 153-164 Available from: URL: <http://www.wjgnet.com/1949-8462/full/v10/i10/153.htm> DOI: <http://dx.doi.org/10.4330/wjc.v10.i10.153>

INTRODUCTION

Congenital coronary artery fistulas (CAFs) are most often incidentally found during coronary angiography (CAG)^[1], computed tomography coronary angiography (CTCA)^[2] and transthoracic echocardiography (TTE)^[3-5]. Coronary artery vascular and cameral fistulas are not only seen in humans, but are also occasionally observed in other mammals^[6]. CAFs are classified as anomalies of termination^[7]. Several diagnostic modalities are available for the morphological and functional detection of CAFs, including physical examination (presence of a continuous murmur), non-invasive methods such as echocardiography^[8,9], myocardial perfusion imaging (MPI)^[10,11], CTCA^[3,9,12] and cardiovascular magnetic resonance imaging (MRI)^[13], invasive techniques such as right heart catheterization, CAG and fractional flow reserve (FFR)^[1,14-18], and incidental detection during positron emission tomography computed tomography (PET-CT)^[19,20]. Exercise and pharmacological PET-CT is commonly applied for the assessment of myocardial perfusion and ischemia, and for the diagnosis and risk stratification of ischemic coronary artery disease (CAD)^[21,22]. Adenosine ¹³N-ammonia PET-CT is useful for assessing coronary flow reserve and myocardial perfusion for risk stratification in patients with CAD^[23], the results of which influence patient management strategies^[24]. Myocardial ischemia can also be detected using single-photon emission computed tomography (SPECT) in patients with congenital CAFs^[15]. It is unclear whether congenital fistulas are associated with reduced myocardial perfusion, which is sometimes associated with impaired left ventricular function. Indications for surgical intervention or percutaneous therapeutic embolization are based on the patient's clinical presentation and on imaging findings. The aim of the present study was to evaluate the value of adenosine pharmacological stress ¹³N-ammonia PET-CT in a selected population of patients with incidentally identified congenital CAFs.

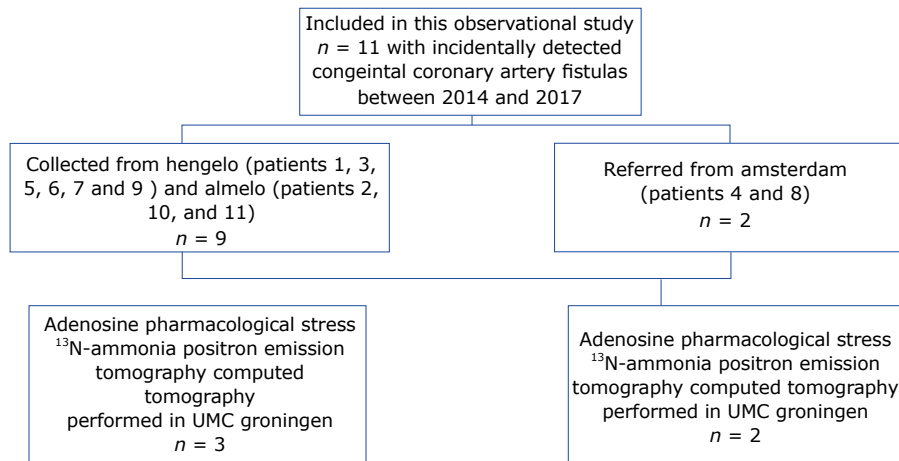


Figure 1 Flowchart of the study patients who were collected from 3 different non-academic Dutch institutes.

MATERIALS AND METHODS

Study subjects

We collected 11 patients (six males and five females; mean age of 64.3 years, range 41-81 years) with CAFs which were incidentally detected during routine CAG between 2014 and 2017. The FFR was not determined due to a lack of facilities. The patients were collected from three centers in the Netherlands as follows: Amsterdam, patients 4 and 8; Hengelo, patients 1, 3, 5, 6, 7 and 9; and Almelo, patients 2, 10 and 11 (Figure 1). Patient data was obtained from the databases of three Dutch cardiac catheterization laboratories (Slotervaart Hospital, Amsterdam; Onze Lieve Vrouwe Gasthuis, Amsterdam; and Hospital Group Twente, Almelo-Hengelo).

All patients underwent electrocardiography (ECG) and TTE. Five patients were further analyzed by adenosine stress/rest ^{13}N -ammonia PET-CT to quantify myocardial blood flow (MBF), myocardial perfusion and coronary flow reserve. Further studies to clarify the clinical presentation and fistula characteristics were performed at the clinician's discretion. Stress and rest MPI SPECT (Symbia S, Siemens Medical Solutions, Erlangen, Germany) were performed in one patient (patient 7), CTCA and MRI were performed in two patients (patients 2 and 4), and shunt calculation by the oximetric method was performed in four patients (patients 3, 4, 7 and 8).

The ECG-gated PET images were acquired using a whole-body 64-slice PET-CT scanner (Biograph True Point; Siemens Medical Solutions). The PET data were acquired in 3D list mode. Patients were studied after an overnight fast, and all refrained from caffeine-containing beverages or theophylline-containing medications for 24 h before the study. Myocardial perfusion was assessed at rest and during vasodilator stress induced by adenosine, using ^{13}N -ammonia as the perfusion radiotracer. Two CT-based transmission scans (120 kVp; 20–30 mA; helical scan mode with a pitch of 1.35) were obtained before and after the resting perfusion studies, performed with

normal breathing to correct for photon attenuation of PET. The procedure involved the intravenous administration of 400 MBq of ^{13}N -ammonia during rest and 400 MBq of ^{13}N -ammonia during adenosine-induced pharmacological stress.

The PET and SPECT images were interpreted semi-quantitatively using the standard American Heart Association 5-point scoring system^[25], and traditional metrics including summed difference score, summed stress score and summed rest score (SRS) were calculated. The SRS (in a fixed perfusion defect) was considered to be a measure of the extent and severity of a previous myocardial infarction (MI). Quantitative MBF values (mL/g per minute) at rest and under stress were computed for each sample on the polar map, as described previously^[21], using a three-tissue compartment pharmacokinetic model for ^{13}N -ammonia^[26]. Myocardial perfusion reserve (MPR) was calculated as the ratio between stress MBF and rest MBF (making it a unitless variable). The resting MBF was corrected for the rate-pressure product. The global MPR and stress MBF were calculated for the whole left ventricular region (defined by the left ventricle long-axis plane), representing the parameters of interest for our analysis.

The ECG-gated images were analyzed using the QGS software package (Cedars-Sinai, Los Angeles, CA, United States)^[27]. Short-axis images were processed, and ventricular edges and cavity volumes were calculated for each of the eight re-binned dynamic frames that were reconstructed for the average cardiac cycle. The algorithm for determining edges and calculating volume has been described previously.

Ethical considerations

The study was reviewed and approved by the local medical ethical committee of the eastern region, Enschede, the Netherlands (ID METC: K18-14, METC /18082.sai). As the patients' personal information was protected, and therefore could not be identified and anonymized, it was exempt from consent by the local medical ethical

Table 1 Symptoms, clinical presentation and physical findings of adult subjects with congenital coronary artery fistula

Case	Fistula origin and termination	Symptoms and clinical presentation	Previous history and risk factors	Physical findings	BMI	Intervention
1	RCA and LAD to PA	Chest pain NSTEMI/PMI (CK 390 U/L)	Tubular adenoma of sigmoid, celiac disease	Normal	32.7	None
2	LAD to PA	Chest pain NSTEMI (CK 573 U/L)	Old IMI Asthma	Normal	25.9	CABG and surgical closure of the fistula
3	LCx to PA	Chest pain	Blanco	Normal	26.6	Coiling of the fistula and PCI of LAD
4	RCA to CS	Dyspnea on exertion	Diaphragmatic hernia, asthma and hypertension	Systolic ejection murmur grade 2/6 2 d ICS	28.2	None
5	LAD to PA	Non-sustained VT	DM, COPD, hypertension, hypothyroidism	Systolic ejection murmur grade 2/6 2 d ICS	33.4	PCI of OM branch and FFR of LAD. Coiling of the fistula
6	LAD to PA	Dyspnea on exertion	COPD Severe mitral valve regurgitation	Apical mitral regurgitation murmur grade 2/6	25.5	Mitral valve plasty
7	LAD to PA	Chest pain	Celiac disease	Normal	24.2	
8	LAD to PA	Angina pectoris	Hypercholesterolemia Positive family history for CAD	Systolic ejection murmur grade 2/6 2 d ICS	21.1	PCI of LAD
9	LCx to PA	Palpitation PAF and non-sustained VT Hypertension	Ischemic CVA	Normal	24.8	None
10	LAD to PA	Angina pectoris	NSTEMI 2010 (CK 328 U/L). PCI of RCA 2012	Normal	24.2	Coiling of the fistula
11	LAD to PA	Chest pain	Hypertension, hypercholesterolemia Positive family history for CAD Smoker	Normal	29.1	None

BMI: Body mass index; CABG: Coronary artery bypass grafting; CAD: Coronary artery disease; CK: Creatinine kinase; COPD: Chronic obstructive pulmonary disease; CS: Coronary sinus; CVA: Cerebral vascular disease; DM: Diabetes mellitus; FFR: Fractional flow reserve; ICS: Intercostal space; IMI: Inferior wall myocardial infarction; LAD: Left anterior descending coronary artery; LCx: Left circumflex coronary artery; NSTEMI: Non-ST elevation myocardial infarction; OM: Obtuse marginal branch; PA: Pulmonary artery; PAF: Paroxysmal atrial fibrillation; PCI: Percutaneous coronary intervention; PMI: Posterior myocardial infarction; RCA: Right coronary artery; VT: Ventricular tachycardia.

committee.

Statistical analysis

Categorical data are expressed as numbers with percentages, and continuous data are expressed as means with a range.

RESULTS

This retrospective case series included 11 (Figure 1) patients with 12 congenital coronary vascular fistulas (CVFs). Of those patients, five underwent adenosine pharmacologic stress ¹³N-ammonia PET-CT to assess myocardial perfusion and functionality of the fistula.

Clinical presentations and features (Table 1) included limited posterior MI (patient 1), angina pectoris and chest pain ($n = 6$), dyspnea on exertion ($n = 3$) and asymptomatic abnormal resting ECG ($n = 1$). One patient (patient 9) presented with palpitation, transient ischemic attack, paroxysmal atrial fibrillation and non-sustained ventricular tachycardia. Previous MI was reported in two patients (patients 2 and 10). Patient 5 had exercise-

induced non-sustained ventricular tachycardia. Physical examination was unremarkable in seven patients. Apical systolic murmur was heard in one patient, and systolic ejection murmur was heard in the second intercostal space in three patients.

In regard to the ECG, sinus rhythm was present in 10 patients and permanent atrial fibrillation was found in one patient. We also observed tall R-waves in precordial lead 2 ($n = 1$), signs of previous inferior MI ($n = 1$), non-specific repolarization abnormalities ($n = 4$), left bundle branch block ($n = 1$), left axis deviation ($n = 1$) and 1st degree atrioventricular delay ($n = 1$).

Echocardiography revealed normal findings in four patients, inferolateral hypokinesia in one patient, anteroseptal akinesia in one patient, mild aortic valvular stenosis with moderate aortic regurgitation (AR) in one patient, mild AR in one patient, mild mitral regurgitation (MR) in three patients, moderate to severe MR in one patient, and mild tricuspid regurgitation in three patients. Right ventricular systolic pressure was normal in all patients. Dilated coronary sinus (CS) was found in one patient (patient 4). One patient underwent

Table 2 Angiographic characteristics of fistula components

Case	Fistula origin and termination	Yr of detection	Angiographic characteristics of fistula components								
			O	LCx	T	O	RCA	T	O	LAD	T
1	RCA and LAD to PA	2014		P		M	MT	M	S	MT	S
2	LAD to PA	2015							M	MT	M
3	LCx to PA	2015	S	ST	S						
4	RCA to CS	2015				S	ST	S			
5	LAD to PA	2016							S	ST	S
6	LAD to PA	2016							M	M	M
7	LAD to PA	2016							M	MT	M
8	LAD to PA	2015							M	MT	S
9	LCx to PA	2016	M	MT	M						
10	LAD to PA	2017							M	M	M
11	LAD to PA	2017							M	MT	S

CS: Coronary sinus; LAD: Left anterior descending coronary artery; LCx: Left circumflex coronary artery; RCA: Right coronary artery; PA: Pulmonary artery; M: Multiple; MT: Multiple and tortuous; S: Single; ST: Single and tortuous; T: Termination; O: Origin; P: Pathway.

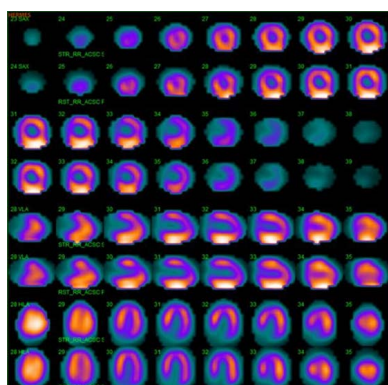


Figure 2 ^{99m}Tc-sestamibi single-photon emission computed tomography scintigraphy, demonstrating normal myocardial perfusion and a normal left ventricular ejection fraction.

^{99m}Tc-sestamibi SPECT scintigraphy (patient 7), which revealed normal myocardial perfusion (Figure 2) and a normal left ventricular ejection fraction (LVEF) of 0.67. Two patients underwent CTCA (patient 2, patient 4), which confirmed the diagnosis of coronary artery vascular fistulas.

Cardiovascular MRI was performed in two patients (patients 2 and 4), which revealed moderate left ventricular hypertrophy and signs of healed MI in three flow territories (patient 2). Shunt calculation by oximetry was performed in four patients (patients 3, 4, 7 and 8) who showed left-to-right shunt ratios of 1.75:1, 1.3:1, 1.1:1 and 2.0:1, respectively, with a mean of 1.53:1 (range 1.1-2.0).

CAG was used to delineate the characteristics of the fistula (origin, pathway and termination; Figures 3-10 and Table 2). The multiplicity of the origin of the fistulous vessels and the pathway were plural in most fistulas (8/12, 67% and 9/12, 75%, respectively). The termination was equally distributed between single (6/12, 50%) and multiple (6/12, 50%) fistulous vessels. Multiplicity was common among the different fistula components (23/36, 64%). Tortuosity of the

pathway was found in eight fistulas (8/12, 67%).

There were 10 unilateral (Figure 4) and one bilateral (Figure 3A and B) fistulas. All fistulas were of the coronary vascular type, terminating into the pulmonary artery (PA, $n = 11$; Figure 5) or the coronary sinus ($n = 1$; Figure 6), and originating from the left anterior descending coronary artery (LAD; $n = 8$; Figure 7), right coronary artery (RCA; $n = 2$; Figures 3B and 6) or left circumflex coronary artery (LCx; $n = 2$; Figures 5 and 10). The characteristics of the fistula (origin, pathway and termination) showed multiple origins of fistulous vessels and pathways in most fistulas (8/12, 67% and 9/12, 75%, respectively; Figure 9). Multiplicity was common among the different fistula components (22/36, 61%; Figures 3B, 4 and 10). In contrast, single (7/12, 58%) termination of the fistulous vessels was more common than multiple (5/12, 42%) termination of fistulous vessels.

Dilated RCA was found in one patient (patient 4; Figure 6A), while large and small aneurysmal formation was present in two patients (patients 2 and 6, respectively; Figures 4 and 8). The FFR was not measured. The ECG-gated imaging of adenosine stress/rest ¹³N-ammonia PET-CT (Table 3) demonstrated homogenous distribution of perfusion in two patients, who showed no perfusion defects (patients 3 and 11). One patient showed diffuse, reversible reductions in perfusion in the apical and antero-septal regions, and partly in the basal anterior segment (patient 4) (Figure 11). In another patient, perfusion of the LAD area was slightly lower than the inferior segment, but it was equal to that of the lateral wall (patient 7). Normal perfusion with reduced LVEF (rest 33% and stress 39%) was probably underestimated in one patient (patient 8). In the five patients, the mean global stress/rest ratio for MPR was 2.9 (range 2.33-3.90). The mean regional stress/rest ratio was 3.0 for the LAD (range 2.35-4.50), 2.9 for the RCA (range 2.49-3.60) and 2.8 for the LCx (range 2.36-3.20). Blood flow through the LAD was slightly higher than flow through the RCA and LCx.

Table 3 Pharmacological adenosine stress/rest ¹³N-ammonia positron emission tomography computed tomography in 5 patients with unilateral coronary vascular fistulas

Case	CAF	Stress/rest perfusion segments				LVEF (%)		Semi-quantitative findings	CAD	Prior procedure	Management of CAF
		LCx	RCA	LAD	Global	Rest	Stress				
3	LCx-PA	2.74	2.49	2.56	2.59	52	57	No perfusion defects	1-VD	PCI-LAD	PTE
4	RCA-CS	2.65	2.7	2.71	2.69	65	65	Diffuse reversible reduction of perfusion in the apical, antero-septal and partially in basal anterior segment	None	None	CMM
7	LAD-PA	2.36	2.55	2.35	2.33	60	65	Perfusion of LAD area is less than inferior segment	None	None	CMM
8	LAD-PA	3.02	2.91	2.94	2.95	33	39	Normal perfusion with reduced LVEF	1-VD	PCI-LAD	CMM
11	LAD-PA	3.2	3.6	4.5	3.9	65	65	No perfusion defects	None	None	CMM

CAD: Coronary artery disease; CAF: Coronary artery fistula; CMM: Conservative medical management; CS: Coronary sinus; LAD: Left anterior descending coronary artery; LCx: Left circumflex coronary artery; LVEF: Left ventricular ejection fraction; PA: Pulmonary artery; PCI: Percutaneous coronary intervention; PTE: Percutaneous transcatheter embolization; RCA: Right coronary artery; VD: Vessel disease.

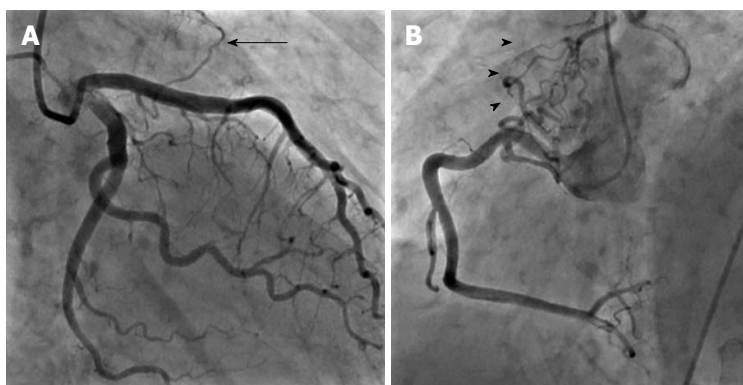


Figure 3 Bilateral fistulas. A: Bilateral fistulas from the left anterior descending coronary artery to the pulmonary artery with single origin, multiple pathway and single termination (arrow); B: Bilateral fistulas from the right coronary artery to the PA with multiple origin, pathway and termination (arrowheads).



Figure 4 Fistula from the proximal left anterior descending coronary artery to pulmonary artery with multiple origin, pathway and termination associated with large aneurysmal formation (arrow).

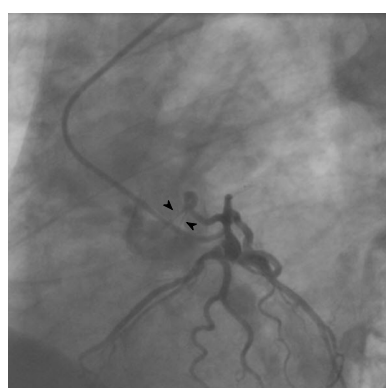


Figure 5 Fistula from the proximal left circumflex artery ending into the pulmonary artery characterized with single origin, pathway and termination emptying with double jets (arrowheads) ending into the pulmonary artery.

Absolute flow quantification in one patient (patient 3) yielded normal myocardial perfusion with high flow in the LCx, which was the fistula-related vessel, when compared to RCA and LAD flow, confirming successful percutaneous transcatheter embolization (PTE) closure of the fistulous vessel. On the other hand, semi-

quantitative analysis revealed normal perfusion in two patients and a diffuse reduction in perfusion in the other two patients. When combined with the semi-quantitative results, findings of normal flow by PET-CT indicate that conservative medical management (CMM) can be used as a management option for fistulous

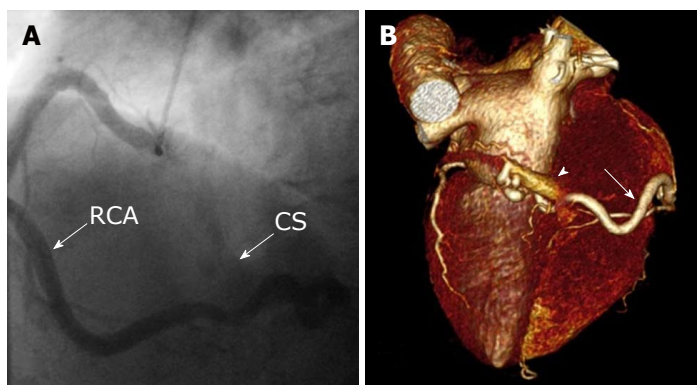


Figure 6 Unilateral fistula and computed tomography coronary angiography. A: Unilateral fistula originating from the right coronary artery (RCA) terminating into the coronary sinus (CS) with single origin, pathway and termination with dilated RCA and enlarged CS; B: Computed tomography coronary angiography: Coronary artery fistula originating from the distal segment of RCA (arrow) and terminating into the coronary sinus. Volume-rendered three-dimensional image reconstruction demonstrating fistulous vessel located posterior connected with the CS (arrowhead). RAC: Right coronary artery; CS: Coronary sinus.

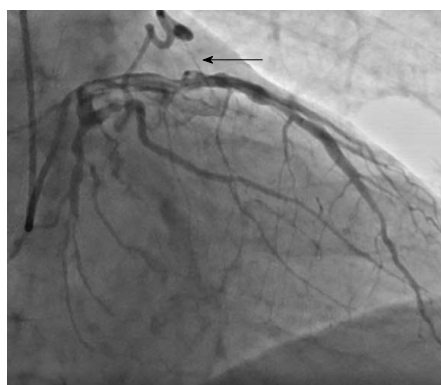


Figure 7 A fistulous connection between the left anterior descending coronary artery and pulmonary artery with single origin, pathway and termination with a single jet ending into the pulmonary artery (arrow).



Figure 9 Left lateral frame demonstrating a fistula with multiple origin (arrow) and pathway from the proximal left anterior descending coronary artery ending to the pulmonary artery with a single termination. O: Origin; P: Pathway; T: Termination.



Figure 8 Right anterior oblique view shows the fistulous vessel between the left anterior descending coronary artery and the pulmonary artery with multiple origin, pathway and termination with small aneurysmal formation (arrow).



Figure 10 Left anterior oblique view shows a fistula between proximal left circumflex coronary artery (arrow) with multiple origin, pathway and termination with outflow to the pulmonary artery.

vessels, thereby avoiding the need for occlusion of the fistula.

The interventions included leaving a small fistula without percutaneous or surgical intervention; surgical ligation (SL) of the fistula in combination with CABG (patient 2); percutaneous closure of the fistulous tract

(LCx to PA) and percutaneous coronary intervention (PCI) of the LAD due to chest pain and dyspnea upon exertion (patient 3); PCI of the OM branch of the LCx and coiling of the fistula (LAD to PA) in a patient (patient 5) with non-sustained ventricular tachycardia; and transcatheter obliteration of the fistula secondary to

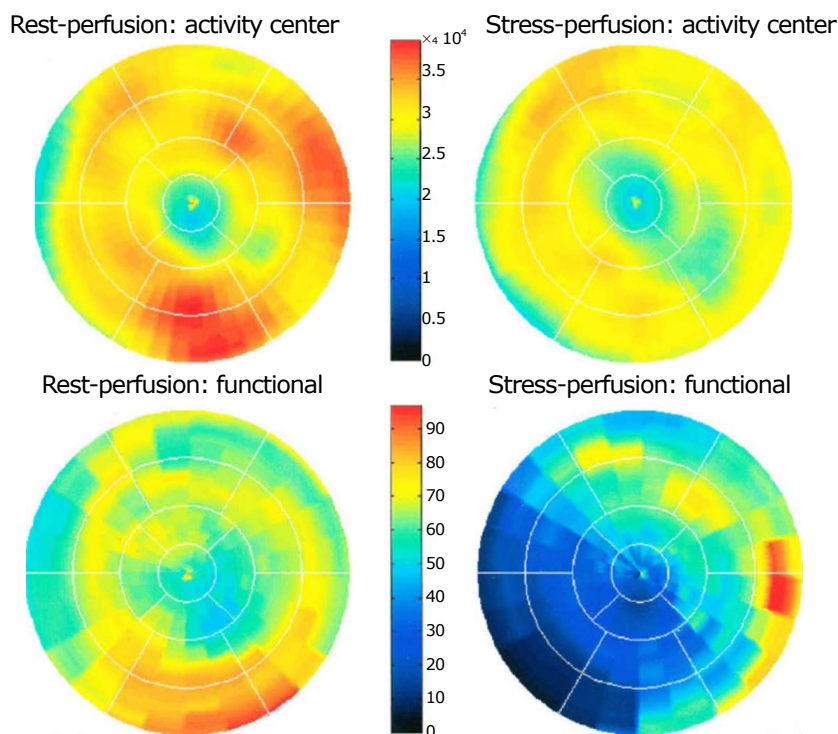


Figure 11 Positron emission tomography computed tomography scanning demonstrating normal findings on the rest ¹³N-ammonia polar map (left panel) and normal perfusion on adenosine ¹³N-ammonia polar map (right panel). Myocardial perfusion was assessed at rest and during vasodilator pharmacological stress induced by adenosine, using 400 MBq of ¹³N-ammonia as the perfusion radiotracer.

angina pectoris (patient 10).

Treatment and management of the fistula included CMM in seven patients, PTE in three patients and SL combined with coronary artery bypass grafting (CABG) in one patient. Of the patients who underwent adenosine stress/rest ¹³N-ammonia PET-CT, PTE was performed in only one patient (patient 3). This patient showed high flow in the LCx, which was the fistula-related vessel, and PTE was successfully performed with angiographic documentation. In the other four patients (patients 4, 7, 8 and 11), PET-CT showed no flow restrictions, indicating CMM and avoiding the need for fistula closure.

Five patients had known CAD (one vessel disease in four patients and three vessel diseases in one patient). Of these patients, three underwent PCI procedures, one patient was managed with optimal medical treatment, and one patient underwent CABG in combination with fistula ligation.

DISCUSSION

In this study, we describe congenital CAFs that were incidentally found in 11 adult patients during routine CAG. To investigate the functional characteristics of these fistulas, PET-CT was performed at rest and after adenosine pharmacological stress in five subjects. To date, the role of PET-CT has not been extensively studied in adult patients with congenital CAFs.

Congenital CAFs are usually asymptomatic in many

adult patients and are usually incidentally detected during routine CAG for suspected CAD. Over the past century, congenital CAFs associated with continuous cardiac murmur have often been confused with patent ductus arteriosus Botalli^[28,29]. More recently, congenital CAFs have been misdiagnosed as a right atrial myxoma^[30].

Coronary artery vascular and cameral fistulas are increasingly found during echocardiography^[3,31,32], CTCA^[2,33] and diagnostic CAG procedures^[1]. One study reported the diagnosis of a small coronary-pulmonary fistula (CPF) by echocardiography in asymptomatic dizygotic twin infant brothers^[31], suggesting a possible genetic cause of CAFs. Invasive CAG is considered the gold standard for the detection and diagnosis of congenital CAFs; however, non-invasive imaging techniques such as contrast echocardiography^[34], 2D and color Doppler echocardiography, cardiovascular MRI and CTCA provide valuable complementary data for the visualization of fistula components (origin, pathway and termination sites) that are not visible on the CAG^[20,35-37].

FFR

The value of FFR has been emphasized by several authors. Ouyang *et al.*^[38] reported deferral of treatment of the fistula-related artery and tandem intermediate stenosis in a patient with a huge CAF originating from the LAD and draining into the PA based on the findings of FFR. In the case of an adult subject assessed by both FFR and intravascular ultrasound, PCI was performed

for significant stenosis of the LAD, which was the fistula-related artery (LAD-PA), but the congenital fistula remained untouched due to the absence of myocardial ischemia^[18]. In congenital CAFs, the steal phenomenon has been demonstrated by FFR^[17]. Few reports have been published regarding the functional assessment of congenital CAFs (left main PA) in which FFR was used to guide clinical decision-making for intervention. In one of these reports, normal FFR was observed for a patient with concomitant moderate coronary artery stenosis, which led to the deferral of surgical or transcatheter interventions^[39]. Furthermore, Hollenbeck *et al*^[40] demonstrated ischemic changes due to the combination of a moderate LAD stenosis and CVF, which was relieved by PCI. Oh *et al*^[41] assessed the hemodynamic significance of congenital multiple micro-fistulas and coronary cameral fistulas by FFR, which ruled out ischemia. In 2014, Sasi *et al*^[42] assessed CAF using coronary flow reserve (CFR) and FFR. The LCx FFR and CFR were 0.97 and 2.33, respectively, and the LAD FFR of 0.86 was associated with a CFR of 1.56. This patient was treated medically. In 2016, Ito *et al*^[43] successfully performed FFR-guided PCI of an intermediate LAD stenosis associated with CAFs, and the fistula was treated conservatively. Bi-directional flow in the fistula may occur in the left ventricle^[44] and the right ventricle^[45]; however, none of our patients demonstrated bi-directional fistulous flow.

Radionuclide examinations and MPI

In the 1990s, myocardial perfusion scintigraphy SPECT using Tl-201 was performed in some patients to determine fistula-related ischemia. A report by Gupta *et al*^[46] in 1991, followed by Glynn *et al*^[47] in 1994, reported the first case studies documenting the use of thallium-201 perfusion imaging for physiological assessment of CAF (LAD-PA) and as the cause of an exercise-induced reversible thallium-201 perfusion defect in an adult patient^[46,47]. The pharmacological stress MPI SPECT technique may indicate segmental perfusion defects in patients with congenital CPF in the absence of CAD^[11]. In a patient series evaluated by Lee *et al*^[11], 35% of patients with congenital CPF without CAD developed perfusion defects, but the findings were only clinically relevant in 12%.

Adenosine stress-induced ¹³N-ammonia PET-CT uptake in the myocardium is related to perfusion and may offer better assessment of myocardial ischemia. Adenosine stress ¹³N-ammonia PET-CT has several advantages over SPECT, such as higher spatial resolution and sensitivity, absolute quantification, better counting efficiency and improved attenuation correction^[11,24]. In 2011, a report described the application of adenosine ¹³N-ammonia PET-CT in congenital CAFs for the first time^[19].

Adenosine ¹³N-ammonia PET-CT scanning is routinely applied to assess the functional status and quantify flow in patients with CAD^[26,48], which could also be used

in subjects with congenital coronary artery anomalies of origin (*i.e.*, single coronary artery^[49]) and termination (*i.e.*, CAFs^[19]).

Quantification of myocardial perfusion facilitates the high-performance detection and localization of perfusion abnormalities. In the same patient with CAF, PET-CT was reported to show greater areas of ischemic change than ^{99m}Tc-sestamibi scintigraphy^[50]. In a comparative study by Kong *et al*^[20], adenosine stress ¹³N-ammonia PET-CT imaging was shown to have higher diagnostic sensitivity (91% vs 65%) and specificity (89% vs 82%) compared with SPECT using Tc-99m sestamibi, providing better assessment of myocardial perfusion. Thus, MPI may guide decisions regarding which patients will benefit from invasive treatment. Adenosine ¹³N-ammonia PET-CT may prove to be valuable in clinical decision-making for whether to close the fistulous communication based on the presence or absence of distribution abnormalities^[51]. Successful SL of the fistula and reconstruction of the CS was performed in an adult male with a congenital RCA-CS fistula, which was associated with aneurysmal dilatation of the CS and stenosis of the CS ostium^[3]. In the patient series reported by Zhang *et al*^[52], SL of isolated congenital CAFs was related to lower morbidity and mortality associated with residual shunt in 8/47 (17%) patients, two of whom required PTE. Based on the findings of adenosine ¹³N-ammonia PET-CT in our five patients, transcatheter or surgical intervention was avoided in four subjects. In the current series, treatment and management of the fistula included CMM in seven patients, PTE in three patients and SL in one patient.

In conclusion, adenosine ¹³N-ammonia PET-CT is a useful technique that provides additional information for diagnosis and decision-making related to the management of incidentally detected congenital CAFs. The technique may also be useful for determining the functional status of the fistula and may add some clues for clinical decision-making in adult patients with congenital CAFs. Further prospective studies with a large number of patients are warranted.

Limitations of the study

Firstly, the study was retrospective in nature, with patients collected from different cardiac catheterization laboratories in the Netherlands. Secondly, this study contained a small sample size, involving a limited number of patients collected from three centers which used different diagnostic modalities. There is increasing need for a prospective international registry.

ARTICLE HIGHLIGHTS

Research background

Congenital coronary artery fistulas (CAFs) are uncommon coronary artery vascular anomalies which are often incidentally found during coronary angiography (CAG) performed for suspected atherosclerotic coronary artery disease (CAD). Moreover, most asymptomatic patients are diagnosed with CAFs during evaluation for cardiac murmur. Nowadays, congenital

CAFs are increasingly detected due to the widespread use of non-invasive techniques such as echocardiography and computed tomography coronary angiography (CTCA). Functional assessment and determination of the clinical significance of CAFs is of great importance for therapeutic decision-making. The choice of treatment strategy depends on the size and location of the fistula, the magnitude of left-to-right shunt and the characteristics of the fistulous tract. Many diagnostic modalities are currently used to evaluate the functional characteristics of the fistula, including non-invasive methods such as Doppler echocardiography, CTCA and radionuclide angiography, and invasive methods such as right heart catheterization and fractional flow reserve (FFR), among others. In the current study, the role of positron emission tomography computed tomography (PET-CT) is described in an observational setting. We aimed to determine the impact of the fistula on the clinical status of the patient, in addition to whether PET-CT can be used to assess the functional status of the fistula. This information was used to determine the best therapeutic strategy, which included monitoring, conservative medical management (CMM), transcatheter catheter embolization or surgical ligation (SL). In general, echocardiography represents the first diagnostic imaging approach, but it may be limited by an inappropriate acoustic window. Modern echocardiography equipment has greater sensitivity, which explains why congenital CAFs are frequently diagnosed by this method. Echocardiography can be used to diagnose and evaluate the hemodynamic significance, anatomy and physiopathology of CAFs. CTCA is a widely used technique that can be used for morphological and functional analyses, as well as for perfusion studies of CAFs. CTCA allows for comprehensive cardiac evaluation, providing morphological and functional data on coronary circulation and myocardial perfusion status, as well as anatomical images. Electrocardiography (ECG)-gated cardiovascular computed tomography may play an important role in the evaluation of the origin, pathway, termination and morphology of the fistula in relation to the adjacent anatomical structures, as well as cardiac morphology and contractility. Cardiovascular magnetic resonance does not use ionic radiation and plays a crucial role in determining myocardial wall viability, characterizing the myocardial tissue and its morphology, as well as providing detailed data related to cardiac function, estimated blood flow within the fistula and the anatomical characteristics. Myocardial perfusion imaging (MPI) is used to identify abnormalities in cardiac and pulmonary circulation, providing the Qp:Qs ratio is required to diagnose and quantify left-to-right shunt, and to assess myocardial perfusion defects that occur as a result of segmental hypoperfusion caused by the fistula-bearing vessel. Myocardial perfusion single-photon emission computed tomography (SPECT) is used to detect myocardial ischemia and to stratify the risk of experiencing a cardiac event in patients with CAFs. The hemodynamic significance of this modality remains unclear. The closure technique for congenital CAFs will be chosen after thorough diagnostic imaging and functional investigation has been performed to assess the hemodynamic and functional significance of the fistula, its anatomical morphology, and its impact on the clinical status of the patient.

Research motivation

The aim of this study was to review and present the current data on non-invasive and invasive diagnostic methods used to evaluate the anatomical morphology and functional significance of CAFs. Medical imaging is important for assessing the location and size of CAFs.

Research objectives

We assessed the hemodynamic impact of CAFs using ¹³N-ammonia PET-CT imaging under pharmacological adenosine-induced stress and at rest. Future research in a larger group of symptomatic and asymptomatic patients with a greater magnitude of left-to-right shunt is warranted.

Research methods

This was an observational study of 11 subjects with congenital CAFs that had been incidentally found during CAG performed for suspected atherosclerotic CAD. In all patients, physical examination, ECG, echocardiography, chest X-ray and laboratory investigation were performed. The patients were collected from three non-academic hospitals in the West and East regions of the Netherlands. FFR was not measured due to a lack of interventional cardiology facilities in these non-interventional hospitals. Different fistula characteristics were delineated using coronary angiographic imaging techniques. Five subjects underwent pharmacological adenosine stress/rest ¹³N-ammonia PET-CT to

assess the hemodynamic impact of the fistula. PET-CT was performed in a different academic center. PET-CT is considered a superior diagnostic modality as it provides data on the metabolic status of the myocardial tissue.

Research results

The patients involved in this study had a variety of clinical presentations, including limited posterior non-ST-elevation myocardial infarction (MI), angina pectoris and chest pain ($n = 6$), dyspnea upon exertion ($n = 3$), and an asymptomatic presentation with abnormal resting electrocardiogram ($n = 1$). One patient presented with palpitation, ischemic cerebrovascular accident, paroxysmal atrial fibrillation and non-sustained ventricular tachycardia. Another patient presented with exercise-induced non-sustained ventricular tachycardia. Previous MI was reported in two patients. The physical examination was unremarkable in seven patients. Apical systolic murmur was heard in one patient, and systolic ejection murmur was heard in the second intercostal space in three other patients. Although continuous cardiac murmur is usually present in patients with CAF, no continuous murmur was heard in the current group of patients. In this case series, the body mass index of subjects ranged between 21.1 to 33.4 kg/m², with four patients classified as normal weight, five as overweight and two as obese. The electrocardiogram demonstrated sinus rhythm in 10 patients and permanent atrial fibrillation in one patient. Echocardiography revealed dilated coronary sinus in one patient. None of the patients showed pulmonary hypertension, with normal results for right ventricular systolic pressure. There were 10 single-sided and one double-sided fistulas. All fistulas were of the coronary vascular type, terminating into the pulmonary artery ($n = 11$) or coronary sinus ($n = 1$), and originating from the LAD ($n = 8$), right coronary artery (RCA, $n = 2$) or left circumflex coronary artery (LCx, $n = 2$). In regard to the characteristics of the fistula (origin, pathway and termination), the origin and pathway of the fistulous vessels was plural in most fistulas (8/12, 67% and 9/12, 75%, respectively). Multiplicity was common among the different fistula components (22/36, 61%). In contrast, single (7/12, 58%) termination of the fistulous vessels was more common than multiple (5/12, 42%) termination of fistulous vessels. The termination was equally distributed between single (6/12, 50%) and multiple (6/12, 50%) fistulous vessels. Multiplicity was common among the different fistula components (23/36, 64%). Tortuosity of the pathway was found in eight fistulas (8/12, 67%). A dilated RCA was found in one patient, and large and small aneurysmal formation was present in two patients. The presence of tortuosity and multiplicity of the fistulous tract meant that percutaneous intervention would be very challenging. In patient 2, who had symptomatic significant CAD, SL of the fistula was performed in combination with coronary artery bypass grafting. The characteristics of the fistula components in this patient were multiple origin and termination with multiple-tortuous pathways, which meant the percutaneous approach could not be used. In four patients (patients 4, 7, 8 and 11), PET-CT showed no flow restrictions. Thus, CMM could be implemented, avoiding the need for fistula closure either transcatheter or surgically. The adenosine stress/rest ¹³N-ammonia PET-CT performed in five subjects demonstrated homogenous distribution of perfusion in two patients, and no perfusion defects in two patients. One patient showed diffuse, reversible reduction in perfusion in the apical and antero-septal regions, and also partly in the basal anterior segment. In another patient, perfusion of the left anterior descending coronary artery (LAD) area was slightly lower than the inferior segment, but it was equal to the lateral wall. Normal perfusion with reduced left ventricular ejection fraction (rest 33%, stress 39%) was probably underestimated in one patient. In these five patients, the mean global stress/rest ratio was 2.9 (range 2.33-3.90). The mean regional stress/rest ratio was 3.0 for the LAD (range 2.35-4.50), 2.9 for the RCA (range 2.49-3.60) and 2.8 for the LCx (range 2.36-3.20). Blood flow through the LAD was slightly higher than through the RCA and LCx. Absolute flow quantification revealed normal myocardial perfusion with high flow in the LCx, which was the fistula-related vessel, compared to the flow of the RCA and the LAD, indicating successful PTE closure procedure of the fistulous vessel. On the other hand, semi-quantitative analysis revealed normal perfusion in two patients and a reduction in diffuse perfusion in the other two patients.

Research conclusions

The hemodynamic characteristics of incidentally found CAFs are of great importance to guide decision-making for whether to treat patients or perform periodic monitoring. Pharmacological adenosine stress/rest ¹³N-ammonia PET-CT in patients with incidentally found congenital CAFs provided adequate

and clear information regarding the hemodynamic burden of the fistula in this small patient population. For better diagnosis of incidentally found congenital CAFs, pharmacological adenosine stress/rest ¹³N-ammonia PET-CT should be performed as part of the diagnostic imaging work-up. However, this needs to be confirmed in a large, prospective, international study or registry. In the current study, pharmacological adenosine stress/rest ¹³N-ammonia PET-CT was performed in a limited number of adult patients with incidentally found congenital CAFs. This test is achievable in patients with congenital CAFs. That pharmacological adenosine stress-rest ¹³N-ammonia PET-CT in incidentally found congenital CAFs is currently, in this patient population, can provide adequate and clear answer regarding the hemodynamic burden of the fistula and guiding the clinical decision making. For patients with CAFs, multiple imaging modalities are required to assess the anatomical morphology, hemodynamic significance and behavior of the fistula in order to assist in the choice of therapeutic strategy. Angiographic characterization of the individual fistula components (origin, pathway and termination) may help guide the selection of closure technique, either percutaneously or surgically.

Research perspectives

Further studies on a larger number of patients with congenital CAFs (small or large, symptomatic or asymptomatic, treated or untreated) are required to determine the prospective incidence and other characteristics, such as history and long-term outcomes. In 2018-2019, we are planning to initiate an international registry on CAFs (Euro-CAF Survey) to address the diagnostic and therapeutic issues.

ACKNOWLEDGEMENTS

The authors would like to thank the members and staff of the catheterization unit of the Department of Cardiology and the Department of Nuclear Medicine, as well as Mr. Jeroen Geerdink, Hospital System Integrator, for his assistance during the preparation of the manuscript.

REFERENCES

- 1 **Karazisi C**, Eriksson P, Dellborg M. Coronary Artery Fistulas: Case Series and Literature Review. *Cardiology* 2017; **136**: 93-101 [PMID: 27577264 DOI: 10.1159/000447445]
- 2 **Ghaffari S**, Akbarzadeh F, Pourafkari L. Aneurysmal coronary arteriovenous fistula closing with covered stent deployment: a case report and review of literature. *Cardiol J* 2011; **18**: 556-559 [PMID: 21947993 DOI: 10.5603/CJ.2011.0013]
- 3 **Pu L**, Li R, Yang Y, Liu G, Wang Y. Right coronary artery coronary sinus fistula with coronary sinus ostium stenosis. *Echocardiography* 2017; **34**: 1102-1104 [PMID: 28517107 DOI: 10.1111/echo.13559]
- 4 **Bittencourt MS**, Seltman M, Achenbach S, Rost C, Ropers D. Right coronary artery fistula to the coronary sinus and right atrium associated with giant right coronary enlargement detected by transthoracic echocardiography. *Eur J Echocardiogr* 2011; **12**: E22 [PMID: 21186199 DOI: 10.1093/ejehoccard/jeq180]
- 5 **Green T**, Crilley J. Endocarditis and coronary artery fistula: a case report. *Eur Heart J* 2018; 1-4 [DOI: 10.1093/ehjcr/tyt023]
- 6 **Scansen BA**. Coronary Artery Anomalies in Animals. *Vet Sci* 2017; **4**: pii: E20 [PMID: 29056679 DOI: 10.3390/vetsci4020020]
- 7 **Villa AD**, Sammut E, Nair A, Rajani R, Bonamini R, Chiribiri A. Coronary artery anomalies overview: The normal and the abnormal. *World J Radiol* 2016; **8**: 537-555 [PMID: 27358682 DOI: 10.4329/wjr.v8.i6.537]
- 8 **Magro V**, Cacciapuoti F, Cacciapuoti F, Lama D. An unexpected finding in a diabetic patient studied with transthoracic echocardiography. *MOJ Gerontol Ger* 2017; **2**: 00041 [DOI: 10.15406/mojgg.2017.02.00041]
- 9 **Zhang P**, Cai G, Chen J, Wang Y, Duan S. Echocardiography and 64-multislice computed tomography angiography in diagnosing coronary artery fistula. *J Formos Med Assoc* 2010; **109**: 907-912

- [PMID: 21195889 DOI: 10.1016/S0929-6646(10)60138-6]
- 10 **Iskandrian AS**, Kimbiris D, Bemis CE, Segal BL. Coronary artery to pulmonary artery fistulas. *Am Heart J* 1978; **96**: 605-609 [PMID: 263393 DOI: 10.1016/0002-8703(78)90196-5]
 - 11 **Lee SK**, Jung JI, O JH, Kim HW, Youn HJ. Coronary-to-pulmonary artery fistula in adults: Evaluation with thallium-201 myocardial perfusion SPECT. *PLoS One* 2017; **12**: e0189269 [PMID: 29216309 DOI: 10.1371/journal.pone.0189269]
 - 12 **Jani L**, Mester A, Hodas R, Kovacs I, Benedek T, Bajka B, Benedek I. Computed tomography assessment of coronary fistulas. *J Interdisc Med* 2017; **2**: 155-159 [DOI: 10.1515/jim-2017-0052]
 - 13 **Detorakis EE**, Foukarakis E, Karavolias G, Dermitzakis A. Cardiovascular magnetic resonance and computed tomography in the evaluation of aneurysmal coronary-cameral fistula. *J Radiol Case Rep* 2015; **9**: 10-21 [PMID: 26629294 DOI: 10.3941/jrcr.v9i7.2305]
 - 14 **Siddiqi MS**, Sharma AK, Sharma J. Giant left circumflex artery aneurysm with coronary artery fistula. *Open Access J Surg* 2016; **1**: 555-572 [DOI: 10.19080/OAJS.2016.01.555572]
 - 15 **Challoumas D**, Pericleous A, Dimitrakaki IA, Danelatos C, Dimitrakakis G. Coronary arteriovenous fistulae: a review. *Int J Angiol* 2014; **23**: 1-10 [PMID: 24940026 DOI: 10.1055/s-0033-1349162]
 - 16 **Sunil Roy TN**, Sajeev CG, Francis J, Krishnan MN, Venugopal K. Three major coronary artery-to-left ventricular fistula: an unusual cause of a diastolic murmur at the apex. *J Am Soc Echocardiogr* 2006; **19**: 1402.e1-1402.e4 [PMID: 17098147 DOI: 10.1016/j.echo.2006.07.013]
 - 17 **Härle T**, Kronberg K, Elsässer A. Coronary artery fistula with myocardial infarction due to steal syndrome. *Clin Res Cardiol* 2012; **101**: 313-315 [PMID: 22212517 DOI: 10.1007/s00392-011-0405-1]
 - 18 **Ouyang F**, Chen M, Yi T, Wu M, Peng H, Huang H, Huang H, Zhou S. Successful percutaneous coronary intervention for multivessel stenosis complicated by a huge coronary artery fistula with the combined physiology and intracoronary anatomy techniques. *Int J Cardiol* 2015; **192**: 70-71 [PMID: 26000465 DOI: 10.1016/j.ijcard.2015.05.026]
 - 19 **Said SA**, Nijhuis RL, Op den Akker JW, Kimman GP, Van Houwelingen KG, Gerrits D, Huisman AB, Slart RH, Nicastia DM, Koomen EM, Tans AC, Al-Windy NY, Sonker U, Slagboom T, Pronk AC. Diagnostic and therapeutic approach of congenital solitary coronary artery fistulas in adults: Dutch case series and review of literature. *Neth Heart J* 2011; **19**: 183-191 [PMID: 22020997 DOI: 10.1007/s12471-011-0088-2]
 - 20 **Kong EJ**, Cho IH, Chun KA, Won KC, Lee HW, Park JS, Shin DG, Kim YJ, Shim BS. Comparison of clinical usefulness between N-13 ammonia PET/CT and Tc-99m sestamibi SPECT in coronary artery disease. *Nucl Med Mol Imaging* 2008; **5**: 354-361
 - 21 **Knuuti J**. Integrated positron emission tomography/computed tomography (PET/CT) in coronary disease. *Heart* 2009; **95**: 1457-1463 [PMID: 19684196 DOI: 10.1136/hrt.2008.151944]
 - 22 **Beanlands RS**, Chow BJ, Dick A, Friedrich MG, Gulenchyn KY, Kiess M, Leong-Poi H, Miller RM, Nichol G, Freeman M, Bogaty P, Honos G, Hudon G, Wisenberg G, Van Berkem J, Williams K, Yoshinaga K, Graham J; Canadian Cardiovascular Society; Canadian Association of Nuclear Radiologists; Canadian Association of Nuclear Medicine; Canadian Nuclear Cardiology Society; Canadian Society of Cardiac Magnetic Resonance. CCS/CAR/CANM/CNCS/CanSCMR joint position statement on advanced noninvasive cardiac imaging using positron emission tomography, magnetic resonance imaging and multidetector computed tomographic angiography in the diagnosis and evaluation of ischemic heart disease—executive summary. *Can J Cardiol* 2007; **23**: 107-119 [PMID: 17311116 DOI: 10.1016/S0828-282X(07)70730-4]
 - 23 **Herzog BA**, Husmann L, Valenta I, Gaemperli O, Siegrist PT, Tay FM, Burkhard N, Wyss CA, Kaufmann PA. Long-term prognostic value of ¹³N-ammonia myocardial perfusion positron emission tomography added value of coronary flow reserve. *J Am Coll Cardiol* 2009; **54**: 150-156 [PMID: 19573732 DOI: 10.1016/j.jacc.2009.02.069]
 - 24 **Siegrist PT**, Husmann L, Knabenhans M, Gaemperli O, Valenta I, Hoefflinghaus T, Scheffel H, Stolzmann P, Alkadhi H, Kaufmann PA. (13)N-ammonia myocardial perfusion imaging with a PET/CT

- scanner: impact on clinical decision making and cost-effectiveness. *Eur J Nucl Med Mol Imaging* 2008; **35**: 889-895 [PMID: 18057933 DOI: 10.1007/s00259-007-0647-3]
- 25 **Dilsizian V**, Bacharach SL, Beanlands RS, Bergmann SR, Delbeke D, Gropler RJ, Knuuti J, Schelbert HR, Travin MI. PET myocardial perfusion and metabolism clinical imaging. *J Nucl Cardiol* 2009; **16**: 651 [DOI: 10.1007/s12350-009-9094-9]
- 26 **Tio RA**, Dabeshlim A, Siebelink HM, de Sutter J, Hillege HL, Zeebregts CJ, Dierckx RA, van Veldhuisen DJ, Zijlstra F, Slart RH. Comparison between the prognostic value of left ventricular function and myocardial perfusion reserve in patients with ischemic heart disease. *J Nucl Med* 2009; **50**: 214-219 [PMID: 19164219 DOI: 10.2967/jnumed.108.054395]
- 27 **Germano G**, Kiat H, Kavanagh PB, Moriel M, Mazzanti M, Su HT, Van Train KF, Berman DS. Automatic quantification of ejection fraction from gated myocardial perfusion SPECT. *J Nucl Med* 1995; **36**: 2138-2147 [PMID: 7472611]
- 28 **Bogers AJ**, Quaegebeur JM, Huysmans HA. Early and late results of surgical treatment of congenital coronary artery fistula. *Thorax* 1987; **42**: 369-373 [PMID: 3660291 DOI: 10.1136/thx.42.5.369]
- 29 **Biorck G**, Crafoord C. Arteriovenous aneurysm on the pulmonary artery simulating patent ductus arteriosus botalli. *Thorax* 1947; **2**: 65-74 [PMID: 20252393 DOI: 10.1136/thx.2.2.65]
- 30 **Wen B**, Yang J, Jiao Z, Fu G, Zhao W. Right coronary artery fistula misdiagnosed as right atrial cardiac myxoma: A case report. *Oncol Lett* 2016; **11**: 3715-3718 [PMID: 27284376 DOI: 10.3892/ol.2016.4457]
- 31 **Caputo S**, Sorice N, Sansone R, Simeone D, Caruso V, Russo R, Cicchella N, Izzo A, Saviano C, Casani A, Ciampi Q, Villari B. Echocardiographic diagnosis of coronary artery fistula in both dizygotic twin brothers: environmental mechanism? *J Cardiovasc Med (Hagerstown)* 2017; **18**: 378-380 [PMID: 20404741 DOI: 10.2459/JCM.0b013e328336b5b7]
- 32 **Ganji JL**, Click RL, Najib MQ, Schaff HV, Chaliki HP. Coronary arteriovenous fistula in a patient with aortic valve regurgitation. *Echocardiography* 2013; **30**: E85-E86 [PMID: 23336353 DOI: 10.1111/echo.12072]
- 33 **Pursnani A**, Jacobs JE, Saremi F, Levisman J, Makaryus AN, Capuñay C, Rogers IS, Wald C, Azmoon S, Stathopoulos IA, Srichai MB. Coronary CTA assessment of coronary anomalies. *J Cardiovasc Comput Tomogr* 2012; **6**: 48-59 [PMID: 22264632 DOI: 10.1016/j.jcct.2011.06.009]
- 34 **Hong SM**, Yoon SJ, Rim SJ. Contrast echo-a simple diagnostic tool for a coronary artery fistula. *Korean Circ J* 2012; **42**: 205-207 [PMID: 22493617 DOI: 10.4070/kcj.2012.42.3.205]
- 35 **Latson LA**. Coronary artery fistulas: how to manage them. *Catheter Cardiovasc Interv* 2007; **70**: 110-116 [PMID: 17420995 DOI: 10.1002/ccd.21125]
- 36 **Cademartiri F**, Malagò R, La Grutta L, Alberghina F, Palumbo A, Maffei E, Brambilla V, Pugliese F, Runza G, Midiri M, Mollet NR, Krestin GP. Coronary variants and anomalies: methodology of visualisation with 64-slice CT and prevalence in 202 consecutive patients. *Radiol Med* 2007; **112**: 1117-1131 [PMID: 18080097 DOI: 10.1007/s11547-007-0210-0]
- 37 **Black IW**, Loo CK, Allan RM. Multiple coronary artery-left ventricular fistulae: clinical, angiographic, and pathologic findings. *Cathet Cardiovasc Diagn* 1991; **23**: 133-135 [PMID: 2070401 DOI: 10.1002/ccd.1810230216]
- 38 **Ouyang F**, Wu M, Peng H, Zhang M, Huang H, Chen M, Huang H, Zhou S. Fractional flow reserve, an effective preoperative guideline to a patient with a huge coronary artery fistula and tandem stenosis. *Int J Cardiol* 2015; **199**: 333-334 [PMID: 26233901 DOI: 10.1016/j.ijcard.2015.06.135]
- 39 **Yew KL**, Ooi PS, Law CS. Functional assessment of sequential coronary artery fistula and coronary artery stenosis with fractional flow reserve and stress adenosine myocardial perfusion imaging. *J Saudi Heart Assoc* 2015; **27**: 283-285 [PMID: 26557747 DOI: 10.1016/j.jsha.2015.03.008]
- 40 **Hollenbeck RD**, Salloum JG. Sequential moderate coronary artery fistula and moderate coronary artery stenosis causing ischemia demonstrated by fractional flow reserve and relieved following percutaneous coronary intervention. *Catheter Cardiovasc Interv* 2014; **83**: 443-447 [PMID: 24038764 DOI: 10.1002/ccd.25170]
- 41 **Oh JH**, Lee HW, Cha KS. Hemodynamic significance of coronary cameral fistula assessed by fractional flow reserve. *Korean Circ J* 2012; **42**: 845-848 [PMID: 23323123 DOI: 10.4070/kcj.2012.42.12.845]
- 42 **Sasi V**, Nemes A, Forster T, Ungi I. Functional assessment of a left coronary-pulmonary artery fistula by coronary flow reserve. *Postepy Kardiol Interwencyjnej* 2014; **10**: 141-143 [PMID: 25061466 DOI: 10.5114/pwki.2014.43526]
- 43 **Ito T**, Murai S, Fujita H, Tani T, Ohte N. Fractional flow reserve-guided percutaneous coronary intervention for an intermediate stenosis complicated by a coronary-to-pulmonary artery fistula. *Heart Vessels* 2016; **31**: 816-818 [PMID: 25643760 DOI: 10.1007/s00380-015-0641-9]
- 44 **Chen JP**, Rodie J. Bi-directional flow in coronary-to-left ventricular fistula. *Int J Cardiol* 2009; **133**: e41-e42 [PMID: 18155306 DOI: 10.1016/j.ijcard.2007.08.126]
- 45 **Ono M**, Otake S, Fukushima N, Sawa Y, Ichikawa H, Kagisaki K, Matsuda H. Huge right ventricle-right coronary artery fistula compromising right ventricular function in a patient with pulmonary atresia and intact ventricular septum: a case report. *J Thorac Cardiovasc Surg* 2001; **122**: 1030-1032 [PMID: 11689814 DOI: 10.1067/mtc.2001.116466]
- 46 **Gupta NC**, Beauvais J. Physiologic assessment of coronary artery fistula. *Clin Nucl Med* 1991; **16**: 40-42 [PMID: 1999055 DOI: 10.1097/00003072-199101000-00010]
- 47 **Glynn TP Jr**, Fleming RG, Haist JL, Huntman RK. Coronary arteriovenous fistula as a cause for reversible thallium-201 perfusion defect. *J Nucl Med* 1994; **35**: 1808-1810 [PMID: 7965162]
- 48 **Hasbak P**, Kjær A. 82 Rubidium PET to replace myocardial scintigraphy. *Ugeskr Laeger* 2011; **173**: 567-572 [PMID: 21333256]
- 49 **Said SA**, de Voogt WG, Bulut S, Han J, Polak P, Nijhuis RL, Op den Akker JW, Slootweg A. Coronary artery disease in congenital single coronary artery in adults: A Dutch case series. *World J Cardiol* 2014; **6**: 196-204 [PMID: 24772259 DOI: 10.4330/wjc.v6.i4.196]
- 50 **Said SA**, Nijhuis RL, Akker JW, Takechi M, Slart RH, Bos JS, Hoorntje CR, Houwelingen KG, Bakker-de Boo M, Braam RL, Vet TM. Unilateral and multilateral congenital coronary-pulmonary fistulas in adults: clinical presentation, diagnostic modalities, and management with a brief review of the literature. *Clin Cardiol* 2014; **37**: 536-545 [PMID: 25196980 DOI: 10.1002/clc.22297]
- 51 **Said SA**, Oortman RM, Hofstra JH, Verhorst PM, Slart RH, de Haan MW, Eerens F, Crijns HJ. Coronary artery-bronchial artery fistulas: report of two Dutch cases with a review of the literature. *Neth Heart J* 2014; **22**: 139-147 [PMID: 24464641 DOI: 10.1007/s12471-014-0518-z]
- 52 **Zhang W**, Hu R, Zhang L, Zhu H, Zhang H. Outcomes of surgical repair of pediatric coronary artery fistulas. *J Thorac Cardiovasc Surg* 2016; **152**: 1123-1130.e1 [PMID: 27245418 DOI: 10.1016/j.jtcvs.2016.04.093]

P- Reviewer: Altarabsheh SE, Barik R, Korosoglou G, Petix NR, Uehara Y, Vermeersch P **S- Editor:** Ji FF
L- Editor: A **E- Editor:** Wu YXJ





Published by **Baishideng Publishing Group Inc**
7901 Stoneridge Drive, Suite 501, Pleasanton, CA 94588, USA
Telephone: +1-925-223-8242
Fax: +1-925-223-8243
E-mail: bpgoffice@wjgnet.com
Help Desk: <http://www.f6publishing.com/helpdesk>
<http://www.wjgnet.com>

